

# Orthomode transducer for the new K-band receiver of the 40 m radio telescope

*A. García, Ó. García-Pérez, F. Tercero, G. Gómez, M. Pérez*

**CDT Technical Report 2022-7**

Observatorio de Yebes – Centro de Desarrollos Tecnológicos  
Dirección General del Instituto Geográfico Nacional

*Abstract-* A new K-band receiver for the Yebes 40 m radio telescope is being developed within the framework of the ASTROREC project. This new receiver will replace the current K-band receiver, extending the frequency coverage up to a range between 18.0 and 32.3 GHz. This report presents the development and characterization of the orthomode transducer (OMT) that will be part of such receiver.



August, 2022



# Contents

<b>Contents .....</b>	<b>3</b>
<b>1 Introduction .....</b>	<b>4</b>
<b>2 Design and simulation.....</b>	<b>5</b>
2.1 Specifications .....	5
2.2 Design of the OMT .....	7
<b>3 Manufacturing and measurement .....</b>	<b>12</b>
3.1 Mechanical design and manufacturing.....	12
3.2 Experimental measurements.....	13
<b>4 Conclusion.....</b>	<b>19</b>
<b>References .....</b>	<b>20</b>
<b>Appendix A. Waveguide interfaces .....</b>	<b>22</b>
<b>Appendix B. OMT interfaces .....</b>	<b>23</b>

# 1 Introduction

During the last years, a series of works have been carried out to update the receivers of the Yebes 40 m radio telescope. These include a new CX-band (4.5-9.0 GHz) receiver [1] for the low-frequency branch, and new Q-band (31.5-50.0 GHz) and W-band (72.0-90.5 GHz) receivers [2] for the high-frequency branch of the Cassegrain-Nasmyth antenna.

In the high-frequency branch, along with the aforementioned Q- and W-band receivers, there is a K-band receiver that currently covers a frequency range between 20.5 and 24.5 GHz [3]. The ASTROREC project<sup>1</sup> aims to develop a new K-band receiver with extended bandwidth, covering the frequency range between 18.0 and 32.3 GHz. In the following sections we present the design and characterization of the orthomode transducer (OMT) for such receiver<sup>2</sup>.

---

<sup>1</sup> Ref: PID2019-107115GB-C22, Convocatoria 2019 de Proyectos de I+D+i del Ministerio de Ciencia e Innovación.

<sup>2</sup> A large part of this work has served Alberto García for the publication of his Master's Thesis [10], where the details of the design are compiled in a more extensive and detailed way.

## 2 Design and simulation

### 2.1 Specifications

The OMT is a passive microwave component, connected between the horn feed and the low-noise amplifiers (LNA), which serves to separate the incoming electromagnetic signal into two orthogonal polarization components.

For the particular case of the ASTROREC K-band receiver, it is required an OMT for dual linear polarization and waveguide input and output ports. The main design specifications for the OMT are summarized in Table 2.1.

Parameter	Specification
Polarization	Dual linear
Bandwidth	18.0 – 32.3 GHz <sup>3</sup>
Return loss	<-15 dB
Insertion loss	>-0.5 dB
Isolation between output ports	>30 dB
Cross polarization rejection	>30 dB
Input port interface	1x square waveguide <sup>4</sup>
Output ports interface	2x rectangular waveguides <sup>4</sup>

Table 2.1: Design specifications for the K-band OMT.

The required frequency range does not match with any of a standard rectangular waveguide. The WR-42 (18-26.5 GHz) has the cutoff frequency of the first high-order mode at about 28.1 GHz (inside the band of interest); and the WR-34 (22-33 GHz) has the cutoff frequency of the fundamental mode at 17.3 GHz, which is below but too close to the band of interest, which may hinder the practical design of the component due to strong impedance mismatching effects and higher losses. Therefore, it has been found necessary to define a custom rectangular waveguide in between the dimensions

<sup>3</sup> Initially 18-32 GHz, but subsequently extended to 18.0-32.3 GHz.

<sup>4</sup> See Appendix A for more details.

of the standard WR-42 and WR-34 waveguides. In particular, a waveguide of **9.2 x 4.6 mm** has been chosen for the rectangular ports, whose cutoff frequency for the fundamental mode (TE<sub>10</sub>) is at 16.3 GHz (enough margin up to 18 GHz) and the first higher order modes (TE<sub>20</sub> and TE<sub>01</sub>) appear at 32.6 GHz (just above the band of interest). The comparison of the different waveguides is summarized in Table 2.2.

In the case of the input square waveguide, its dimensions will be **9.2 x 9.2 mm**. In such case, the cutoff frequency of the fundamental modes (TE<sub>10</sub>, TE<sub>01</sub>) is the same than in the rectangular waveguide, but the first higher order modes (TE<sub>11</sub>, TM<sub>11</sub>) would appear at 23.1 GHz, which is in the middle of the band. Fortunately, due to the unequal electric/magnetic symmetry nature of such potentially problematic modes in relation with the fundamental modes, it is possible to avoid mode conversions by choosing an appropriate geometry of the OMT [4]. The mode analysis for both rectangular and square waveguides is shown in Table 2.3.

Rectangular waveguide	Recommended frequency	a (mm) [(inch)]	b (mm) [(inch)]	Cutoff fundamental TE <sub>10</sub>	Cutoff 1 <sup>st</sup> high-order mode
WR-42 standard	18.0–26.5 GHz	10.668 [0.42]	4.318 [0.17]	14.051 GHz	28.102 GHz
<b>Custom 18-32.3 GHz</b>	<b>18.0–32.3 GHz</b>	<b>9.2 mm</b>	<b>4.6 mm</b>	<b>16.304 GHz</b>	<b>32.609 GHz</b>
WR-34 standard	22.0–33.0 GHz	8.636 [0.34]	4.318 [0.17]	17.357 GHz	34.715 GHz

Table 2.2: Comparison between standard waveguides and the proposed custom waveguide for the rectangular waveguide ports.

Rectangular waveguide (9.2 x 4.6 mm)		Square waveguide (4.6 x 4.6 mm)	
Mode	Cutoff freq. (GHz)   norm.	Mode	Cutoff freq. (GHz)   norm.
TE <sub>10</sub> (fundam.)	16.30   1.00	TE <sub>10</sub> , TE <sub>01</sub> (fundam.)	16.30   1.00
TE <sub>20</sub>	32.61   2.00	TE <sub>11</sub> , TM <sub>11</sub>	23.06   1.41
TE <sub>01</sub>	32.61   2.00	TE <sub>20</sub>	32.61   2.00
TE <sub>11</sub> , TM <sub>11</sub>	36.46   2.24	TE <sub>02</sub>	32.61   2.00
TE <sub>21</sub> , TM <sub>21</sub>	46.12   2.83	TE <sub>21</sub> , TM <sub>21</sub>	36.46   2.24
		TE <sub>12</sub> , TM <sub>12</sub>	36.46   2.24

Table 2.3: Analysis of electromagnetic modes for the proposed rectangular and square waveguides.

## 2.2 Design of the OMT

The band of interest (18.0 – 32.3 GHz) corresponds to a relative bandwidth of 1.79:1. As it can be seen from the analysis in Table 2.3, some undesired electromagnetic modes (i.e. TE<sub>11</sub> and TM<sub>11</sub>) can be propagated through the input square waveguide, since their cutoff frequency falls in the middle of the band. Power conversions between the fundamental and higher order modes are generally undesired in the design of OMTs, since it is one of the main limiting factors for its bandwidth. Nevertheless, some mode conversions can be avoided by a proper choice of the OMT topology. According to [4], the OMTs can be classified into 3 categories attending to their geometric symmetries:

- Class I: They are symmetric along a single plane. Consequently, they are simpler to manufacture but more limited in bandwidth (usually less than 1.3:1). Some examples are the T-junction [5] or the finline [6] types.
- Class II: They present two-fold rotational symmetry, so they are more complex structures compared to Class I. However, their particular symmetry properties allow avoiding power transfer between the fundamental and the first higher order modes, which in turn results in a broader achievable bandwidth (up to about 1.8:1). Some examples are the Bøifot [4], the double-ridge [7] or the backward coupler OMTs [8].
- Class III: They present four-fold rotational symmetry, so they require even more complex manufacturing processes. They are equally limited in bandwidth as Class II OMTs, but they have the advantage of providing identical response along the two output branches. A typical example of this type is the turnstile junction [9].

From the options exposed above, the topology chosen for the K-band OMT is the so called **double-ridge** OMT (class II) [7], since we have considered it provides an adequate tradeoff between ease of manufacturing and bandwidth. The double-ridge topology is similar to the traditional Bøifot [4], but incorporates some modifications that simplify the structure and avoid the use of the posts and the vane/septum used in the latter.

The geometry of the designed double-ridge OMT is shown in Fig. 2.1. As it can be seen in the figure, it consists of a common square waveguide input port, and two rectangular waveguide output ports (the three highlighted in red). From now on, the convention to number the ports in this document is as follows: the common square waveguide port is numbered as port 3, the output after combining the two side arms is numbered as port 1, and the output from the forward arm and the E-plane bend is numbered as port 2. The structure has been electromagnetically simulated and optimized using CST Studio [10]. The signal propagation along the OMT has been

depicted in Fig. 2.2, demonstrating the expected performance of the OMT depending on the incoming electric field polarization.

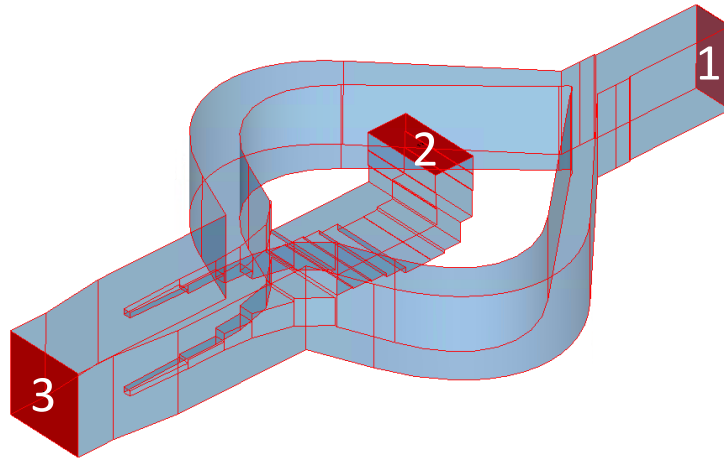


Fig. 2.1: K-band OMT geometry for the electromagnetic simulations in CST.

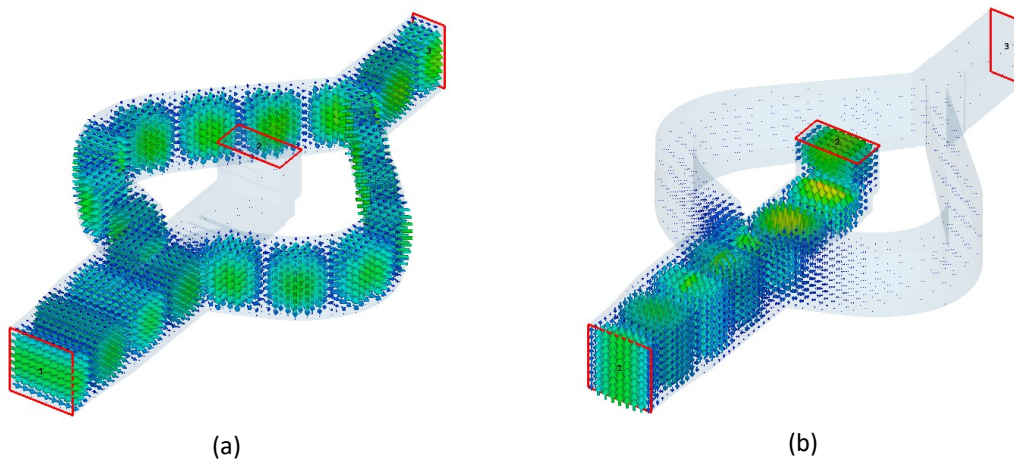


Fig. 2.2: E-field propagation along the OMT for each of the two orthogonal linear polarizations (simulated in CST at 25 GHz).

Following the topology shown in Fig. 2.1, two different designs have been optimized and manufactured. Due to a preliminary bandwidth specification for the OMT between 18-32 GHz, a first design was carried out for such frequency range (denoted as YOMT-K-02) [11]. After a subsequent slight increase of the bandwidth between 18-32.3 GHz, it was found appropriate to introduce minor modifications in the previous design to ensure the adequate performance in the upper part of the extended band (denoted as YOMT-K-03). The simulated S-parameters of both YOMT-K-02 and YOMT-K-03 are plotted in Fig. 2.3 and Fig. 2.4 respectively.



In the case of YOMT-K-02, the reflection coefficients  $S_{11}$  and  $S_{22}$  are better than -18.5 and -18.0 dB respectively in the whole band (18.0-32.3 GHz). Although it fulfills the specifications presented in Table 2.1, this design was initially conceived for a narrower bandwidth, and presents a noticeable peak in the  $S_{22}$  just above (but very close to) 32.3 GHz.

Since the peaks so close to the upper limit of the band can become problematic in practice, due to manufacturing tolerances or thermal effects, a second design was optimized to provide some more margin in the upper part of the band. This second design, denoted as YOMT-K-03, is practically identical to YOMT-K-02 except for a slight widening of the waveguide at the beginning of the two side arms. This design presents reflection coefficients  $S_{11}$  and  $S_{22}$  better than -18.0 and -18.2 dB respectively in the band of interest. In this case the peaks still appear at both ports, but starting at about 32.5 GHz. The rest of parameters of interest (i.e. insertion losses, isolation and cross-polar) that could be extracted from simulation are non-representative due to the use perfect electric conductor (PEC) as base material and the ideal symmetries of the structure in the software.

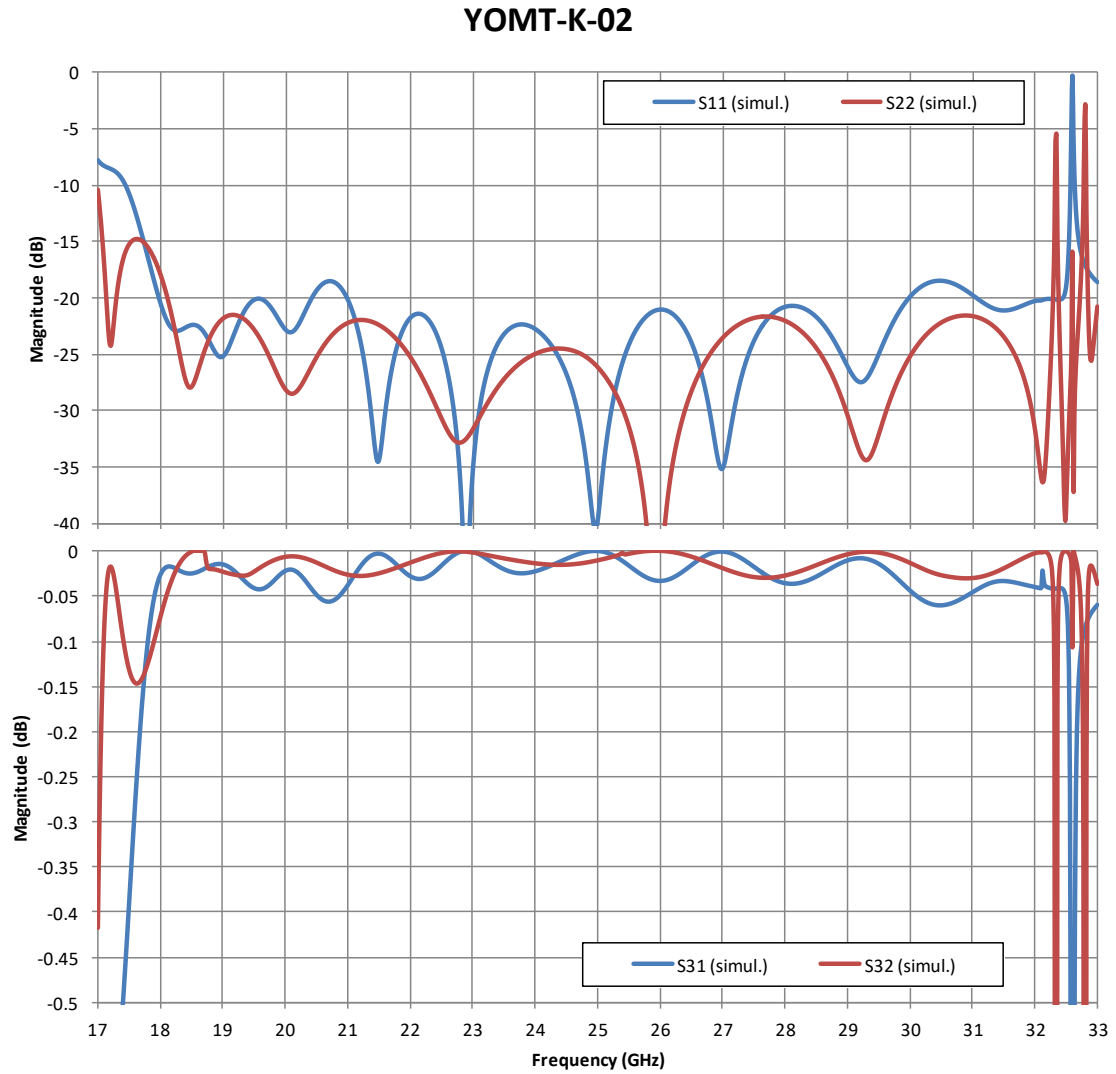


Fig. 2.3: Simulated S-parameters of the first design of K-band OMT (YOMT-K-02).

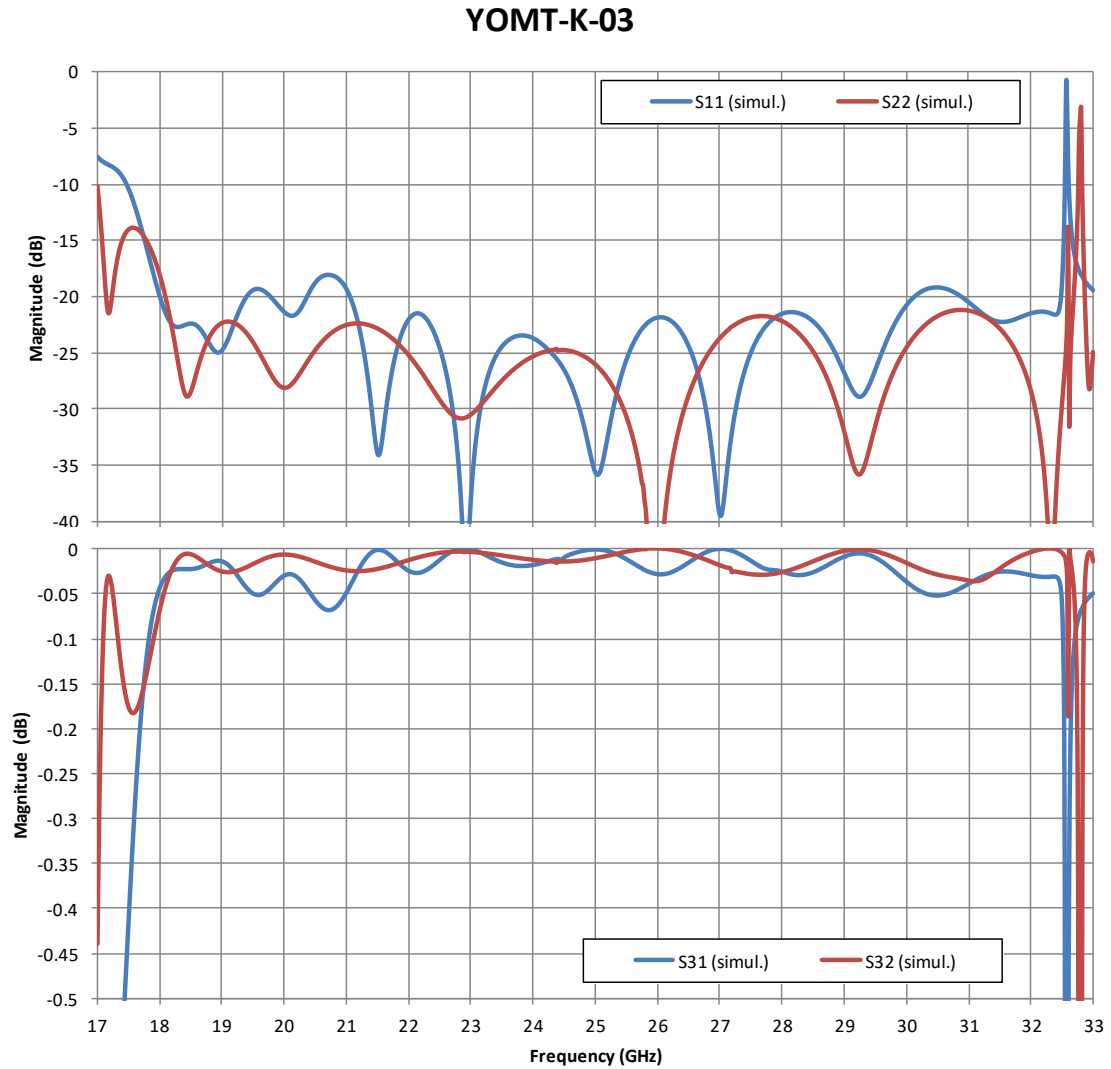


Fig. 2.4: Simulated S-parameters of the second design of K-band OMT (YOMT-K-03).

## 3 Manufacturing and measurement

### 3.1 Mechanical design and manufacturing

One of the advantages of the double-ridge OMT is that it can be easily manufactured from two pieces based on a “split-block” construction. The mechanical models of the designed OMTs have been obtained using Autodesk Inventor [12], and the view of the final 3D model is shown in Fig. 3.1 (see Appendix B for details). The dimensions of the component are 70.0 x 55.0 x 27.2 mm. Due to the use non-standard waveguides, it has been necessary to define the flanges layouts for both square and rectangular waveguides (see Appendix A).

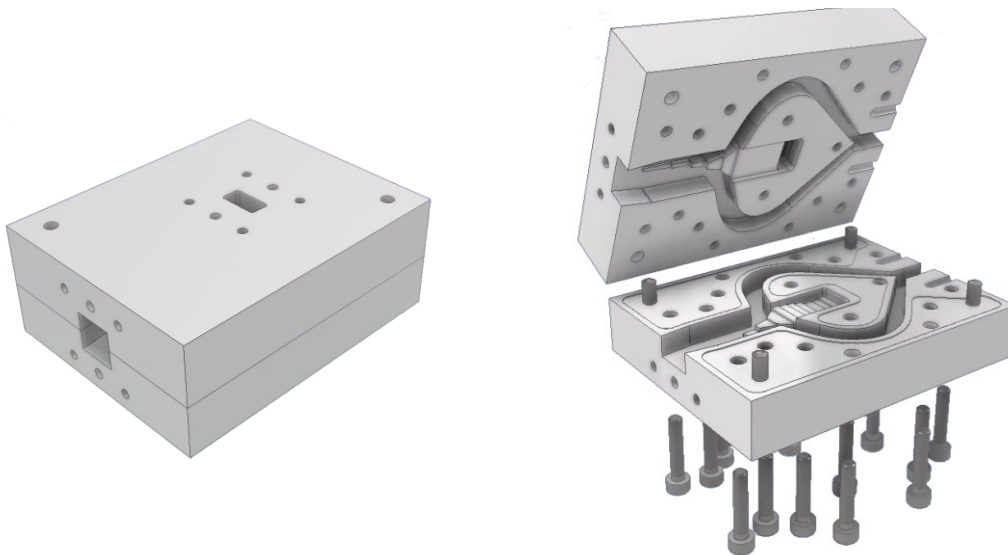


Fig. 3.1: Realistic view of the designed OMT in Autodesk Inventor.

Following the two electric designs presented in Section 2, two OMT units (one of each type, denoted as YOMT-K-02-001 and YOMT-K-03-001 respectively) have been manufactured in aluminum using a 5-axis CNC milling machine (model Mikron S 400 U [13]). The outer dimensions and waveguide interfaces are identical in both cases, so they are fully interchangeable. The only difference is the slight modification in one part of the inner waveguide to correct the resonances seen in the simulation (see Section 2). A picture of the manufactured components is shown in Fig. 3.2.

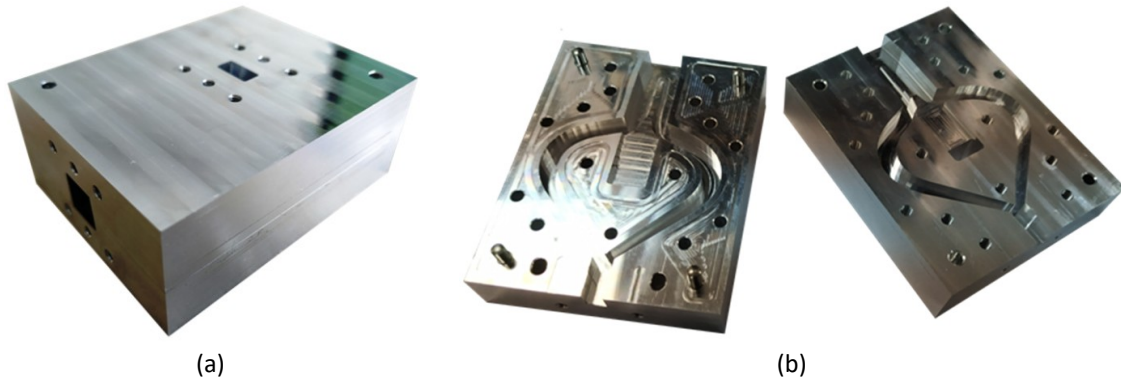


Fig. 3.2: Manufactured OMT: (a) assembly and (b) constituent parts.

## 3.2 Experimental measurements

The S-parameters of both manufactured OMT units have been measured at room temperature using a network analyzer (PNA) model N5225B from Keysight [14]. Since the PNA has two coaxial ports and the OMT has waveguide ports, it has been necessary to construct a set of waveguide transitions and components for the calibration and measurement of the OMTs (see Table 3.1 and Fig. 3.3).

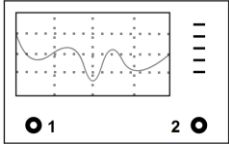
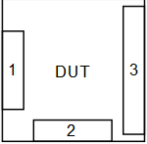
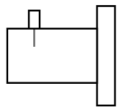
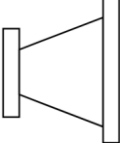




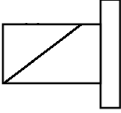
<b>Components for the calibration/measurement of the OMT</b>	
 <p>Vector network analyzer (PNA)</p>	 <p>OMT (device-under-test)</p>
 <p>Coaxial-to-rectangular waveguide transition</p>	 <p>Rectangular-to-square waveguide transition</p>
 <p>Square-waveguide short-circuit</p>	 <p>Square-waveguide quarter-wavelength line</p>
 <p>Rectangular-waveguide short-circuit</p>	 <p>Rect.-waveguide quarter-wavelength line</p>
 <p>Rectangular-waveguide matched load</p>	

Table 3.1: List of components for the calibration and measurement of the OMTs.

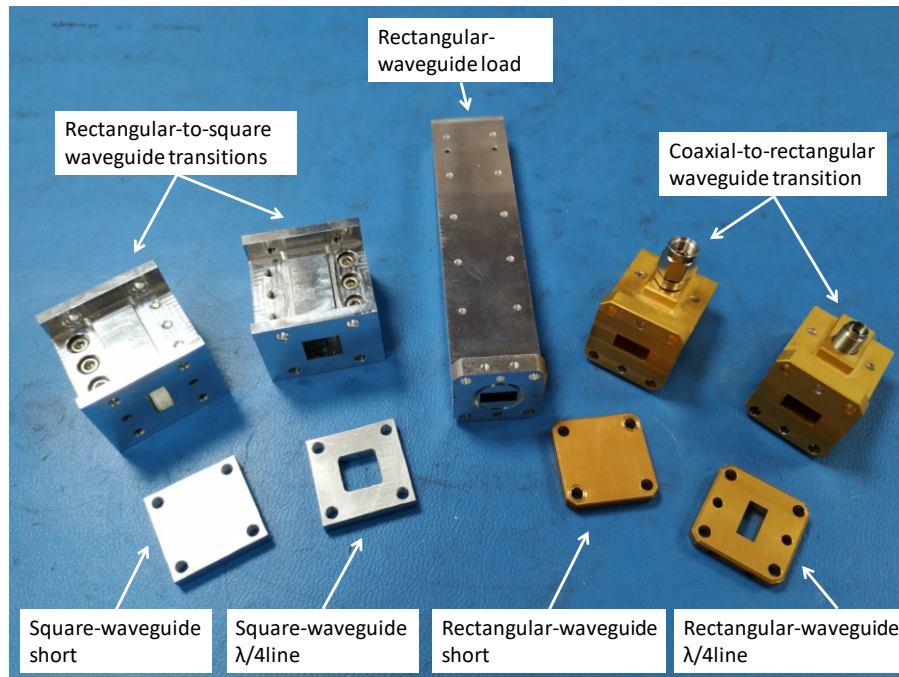


Fig. 3.3: Calibration kit for the measurement of the OMTs.

The calibration of the equipment used for the measurement of the reflection ( $S_{11}$ ,  $S_{22}$ ) and transmission parameters ( $S_{31}$ ,  $S_{32}$ ) is based on the TRL (thru-reflect-line) method with *unknown thru* (in this case, the rectangular-to-square waveguide transition). This procedure consists of 7 steps of calibration, as it is depicted in Fig. 3.4. The measurement of the isolation between the output ports ( $S_{21}$ ,  $S_{12}$ ) would require a simpler calibration method (since the ports 1 and 2 are equal) but it is needed to load the common square-waveguide port with a matched load during the measurement. However, no isolation results are presented in this report due to the unavailability of such load (which can be either a waveguide termination or a horn antenna) during this measurement campaign. Nevertheless, according to our experience, this parameter should not be problematic in practice given the accuracy of the CNC milling machine and the frequency of operation of the OMT. In any case, the isolation will be checked according to the specifications provided in Table 2.1 as soon as the horn antenna is available.

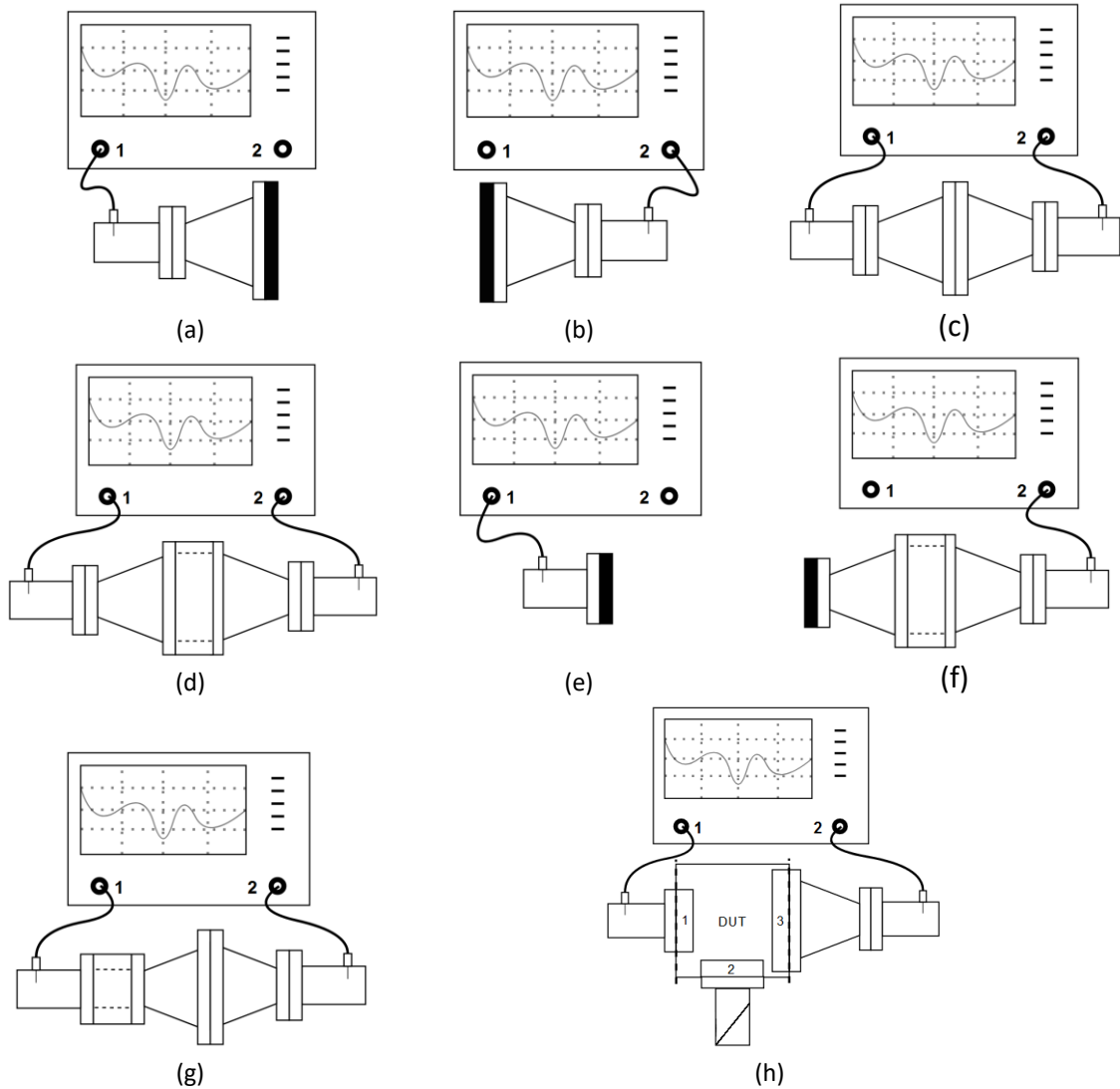


Fig. 3.4: TRL calibration procedure and measurement of the OMT. The reference plane at port1 is at the rectangular waveguide interface after a coaxial-to-waveguide transition, and the reference plane at port 2 is at the square waveguide interface after a coaxial-to-waveguide transition and a rectangular-to-square waveguide transition. Since the interfaces do not match (square and rectangular waveguides), the square-to-waveguide transition is used as “unknown thru”. The calibration steps are as follows: (a) port1 + transition + short, (b) port2 + short, (c) port1 + transition + port2, (d) port1 + transition + line (square) + port2, (e) port1 + short, (f) port2 + line (square) + transition + short (rectangular), (g) port1 + line (rectangular) + transition + port2, and (h) measurement of the OMT (the unused rectangular waveguide port is loaded with the matched load).

The measured S-parameters of the two manufactured OMT units are represented in Fig. 3.5 and Fig. 3.6 respectively. As it can be observed, the return losses agree very well with the results predicted from the electromagnetic simulations of the respective models (see Fig. 2.3 and Fig. 2.4).

In the case of YOMT-K-02-001 (first design), the reflection coefficients S11 and S22 are better than -18.3 and -15.8 dB respectively in the band of interest. The degraded performance at port 2 is given by the high frequency peak that already appeared in the simulation (see Fig. 2.3) and that has approached to the higher limit of the band of interest (32.3 GHz) in the measurement. Nevertheless, the return loss at both ports still fulfills the specifications given in Table 2.1. With respect to the insertion losses, they are about -0.04 and -0.06 dB in average at ports 1 and 2 respectively.

For the YOMT-K-03-001 (second design) it can be observed that the measured response is very similar to the one of the previous unit, but the high frequency peaks are not so close to the band of interest. Consequently, the reflection coefficients S11 and S22 are better than -17.7 and -19.0 dB in the band of interest. On the other hand, the insertion losses are about -0.04 and -0.03 dB in average at ports 1 and 2 respectively. The improved performance of this second unit with respect to the previous one makes it more suitable for its use in the final design of the new K-band receiver.



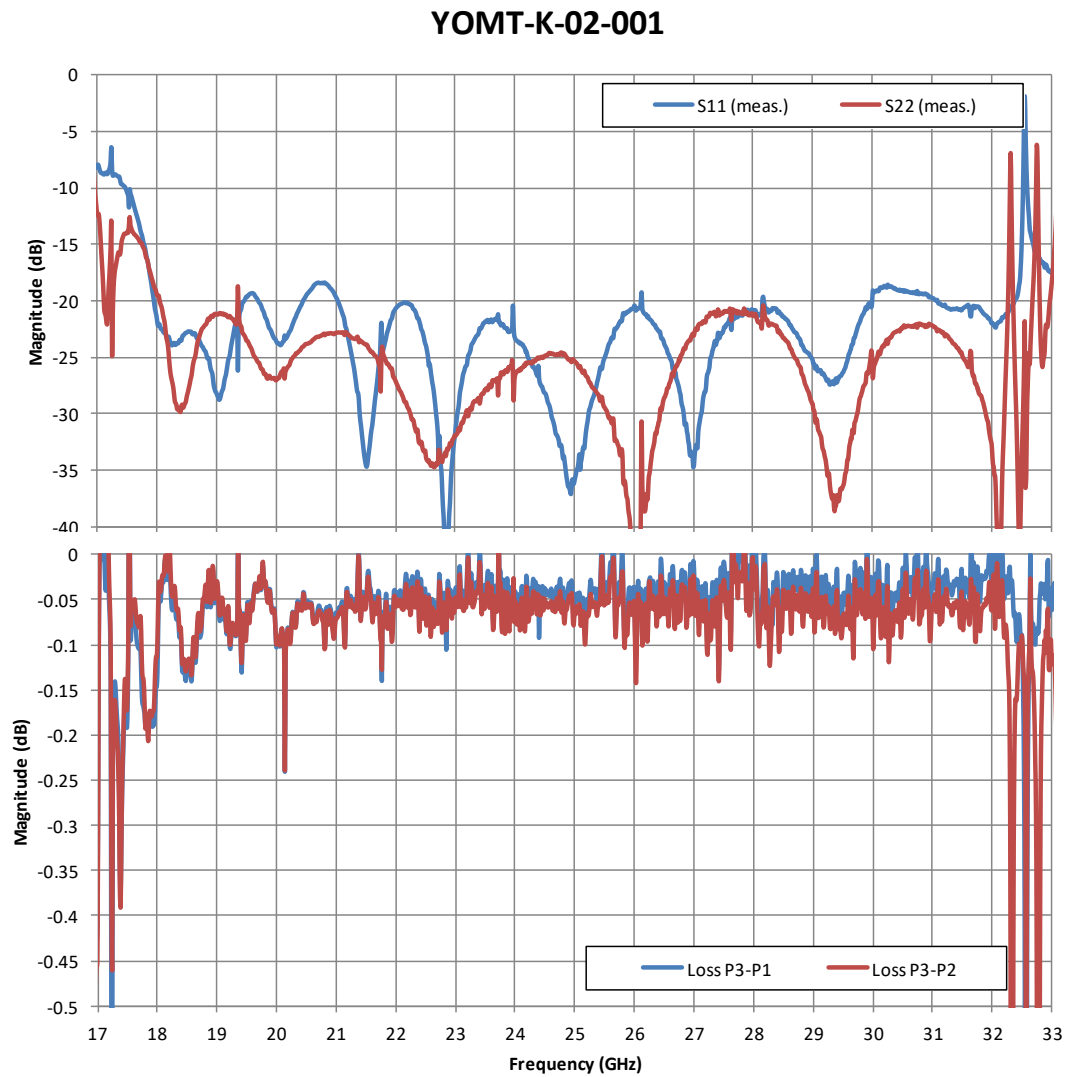


Fig. 3.5: Measured S-parameters of the first design of the K-band OMT (YOMT-K-02-001).

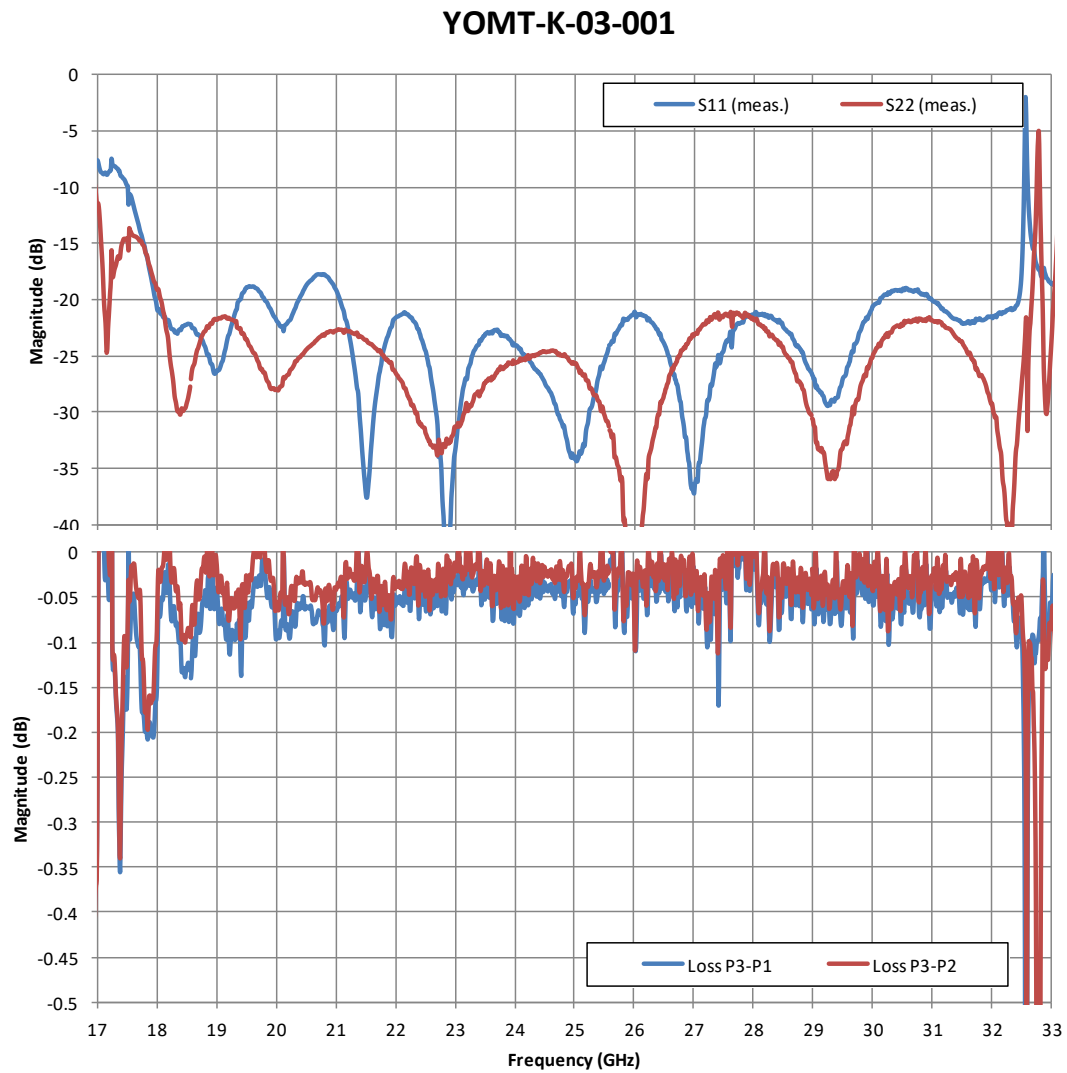


Fig. 3.6: Measured S-parameters of the second design of the K-band OMT (YOMT-K-03-001).

## 4 Conclusion

The development of an OMT for a new K-band receiver at the 40 m radio telescope has been presented. The main challenge for its design has been the required bandwidth (18.0-32.3 GHz), which exceeds the recommended bandwidth for standard rectangular waveguides. The proposed double-ridge topology provides very good electric performance in the whole bandwidth with a structure that is relatively easy to fabricate compared to other alternatives. From the two implemented units, the OMT numbered as YOMT-K-03-001 provides better performance and is the preferred candidate to be installed in the receiver.

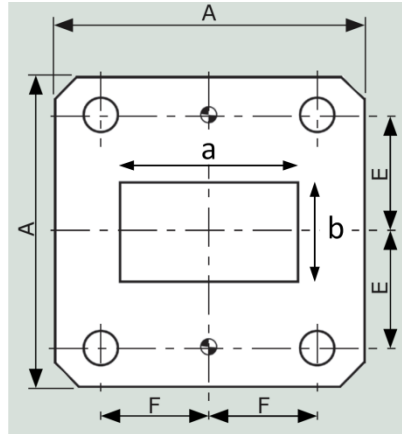
# References

- [1] C. García-Miró and J. Rivero-González, "A new state-of-the-art receiver for Yebes Observatory's 40-metre radio telescope," 22 February 2022. [Online]. Available: <https://jive.eu/cx-receiver-yebes>.
- [2] F. Tercero, J. A. López-Pérez, J. D. Gallego and others, "Yebes 40 m radio telescope and the broad band NANOCOSMOS receivers at 7 mm and 3 mm for line surveys," *Astronomy & Astrophysics*, vol. 645, p. A37, 2021.
- [3] B. Vaquero, F. Tercero, J. A. López-Fernández and others, "New K band receiver for multifrequency VLBI," Technical Report IT-CDT-2015-6, Observatorio de Yebes, 2015.
- [4] A. Boifot, E. Lier and T. Schaug-Pettersen, "Simple and broadband orthomode transducer," *IEE Proceedings H (Microwaves, Antennas and Propagation)*, vol. 137, no. 6, pp. 396-400, 1990.
- [5] O. Garcia-Perez, F. Tercero and S. Lopez-Ruiz, "Orthomode transducer for the new W-band receiver of the 40 m radio telescope," Technical Report IT-CDT-2018-9, Observatorio de Yebes, 2018.
- [6] C. Groppi, C. Y. D. d'Aubigny, A. W. Lichtenberger and others, "Broadband finline transducer for the 750-1150 GHz band," in *Proceedings of the 16th. International Symposium on Space Terahertz Technology*, 2005.
- [7] N. Reyes, P. Zorzi, J. Pizarro and others, "A dual ridge broadband orthomode transducer for the 7-mm band," *Journal of Infrared, Millimeter, and Terahertz Waves*, vol. 33, no. 12, pp. 1203-1210, 2012.
- [8] C. Groppi, A. Navarrini and G. Chattopadhyay, "A waveguide orthomode transducer for 385-500 GHz," *Millimeter, Submillimeter, and Far-Infrared Detectors and Instrumentation for Astronomy V*, vol. 7741, p. 77412D, 2010.

- [9] S. Lopez-Ruiz, F. Tercero, M. G. Nuñez and J. A. Lopez-Fernandez, "31.5 GHz-50.0 GHz ortho-mode transducer for the Nanocosmos receiver in the 40m radiotelescope," Technical Report IT-CDT-2017-1, Observatorio de Yebes, 2017.
- [10] Dassault Systèmes, "CST Studio Suite - Electromagnetic field simulation software," [Online]. Available: <https://www.3ds.com/products-services/simulia/products/cst-studio-suite/>. [Accessed July 2022].
- [11] A. Garcia-Merino, Diseño y modelado de un transductor de modos ortogonales (OMT) criogénico y de banda ancha para aplicación de radioastronomía, M.S. Thesis, Universidad de Alcalá, 2021.
- [12] Autodesk, "Inventor: powerful mechanical design software for your most ambitious ideas," [Online]. Available: <https://www.autodesk.com/products/inventor/overview>. [Accessed July 2022].
- [13] GF Machining Solutions, "Mikron Mill Serie S U," [Online]. Available: <https://www.gfms.com/es-us/machines/milling/5-axis/mikron-mill-s-u-series.html>. [Accessed July 2022].
- [14] Keysight Technologies, "N5225B PNA Microwave Network Analyzer," [Online]. Available: <https://www.keysight.com/us/en/product/N5225B/pna-microwave-network-analyzer-900-hz-10-mhz-50-ghz.html>. [Accessed July 2022].

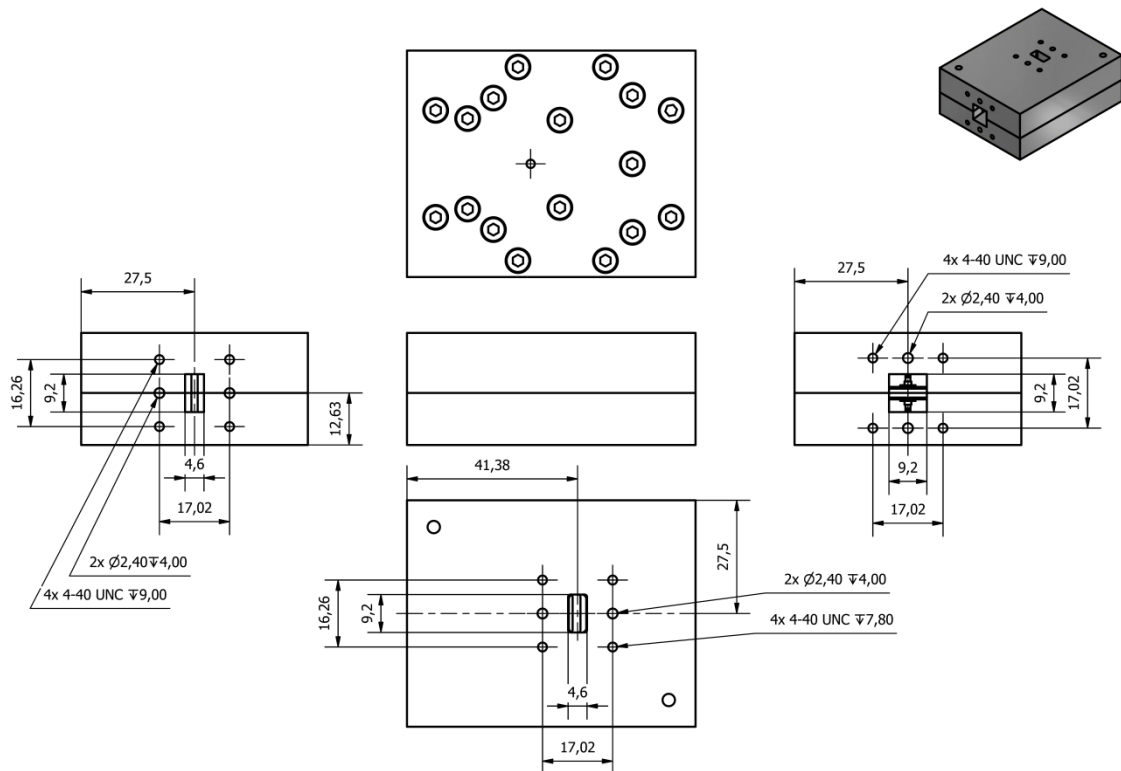
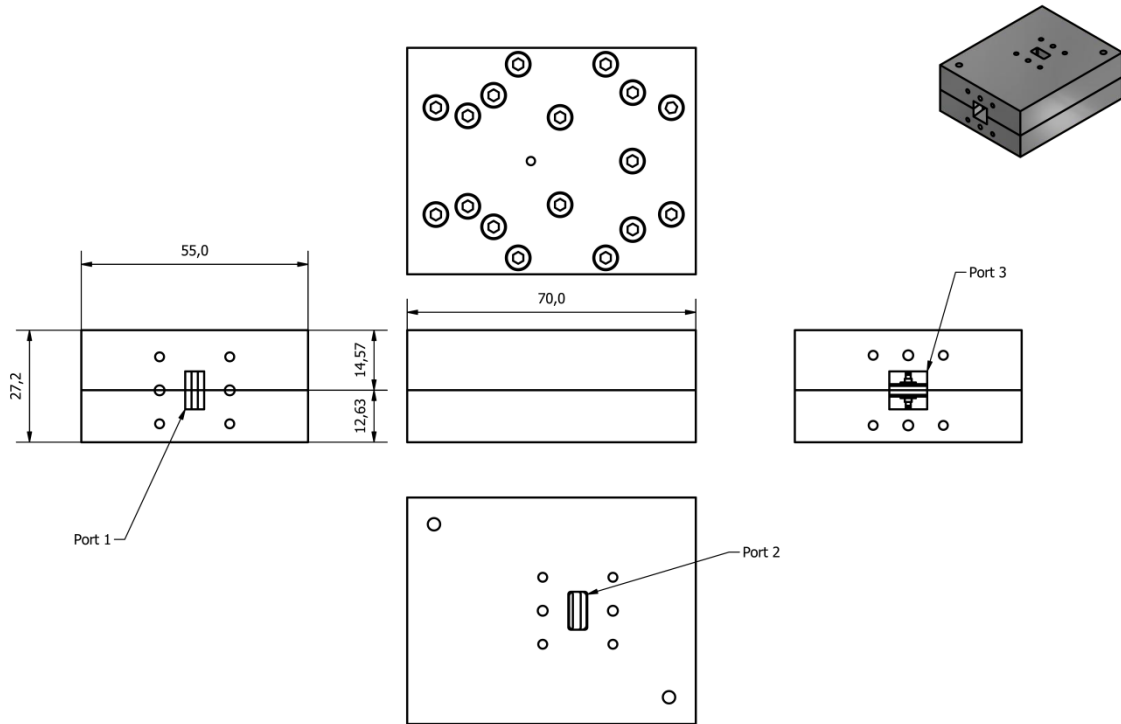
# Appendix A. Waveguide interfaces

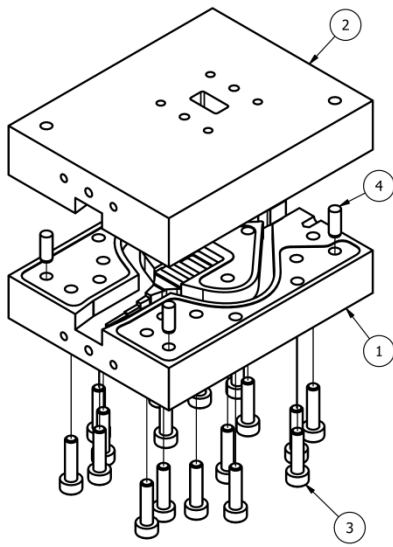
General definition of the custom waveguide interfaces for the new K-band receiver.



Parameter	Rectangular waveguide	Square waveguide
a	9.2 mm	9.2 mm
b	4.6 mm	9.2 mm
A	22.40 mm	22.40 mm
E	8.51 mm	8.51 mm
F	8.13 mm	8.51 mm
Holes	4x 4-40 UNC [4x $\varnothing 2.95$ mm]	4x 4-40 UNC [4x $\varnothing 2.95$ mm]
Dowel holes	2x $\varnothing 2.40$ mm (for 3/32" dowels)	2x $\varnothing 2.40$ mm (for 3/32" dowels)
Thickness	4.75 mm	4.75 mm

# Appendix B. OMT interfaces





LISTA DE PIEZAS			
ELEMENTO	CTDAD	Nº DE PIEZA	DESCRIPCIÓN
1	1	YOMT-K-02-001_parte_inf	Parte inferior OMT banda K
2	1	YOMT-K-02-002_parte_sup	Parte superior OMT banda K
3	17	DIN 912 - M3 x 12	Tornillo de cabeza cilíndrica
4	4	ISO 2338 - 3 m6 x 8 - A	Pasador cilíndrico